Microstructure modeling of various cross-sections of kinked fibers through submicron resolution computed tomography

J. H. Lim[1*], D. W. Kim[1], Y. H. Kim[2] and D. S. Hwang[3]

[1]Division of Mechanical Engineering, Chonbuk National University, Jeonju, Republic of Korea
[2]Korea Advanced Institute of Science and Technology, Daejeon, Republic of Korea
[3]Korea Aerospace research Institute, Daejeon, Republic of Korea

[*]Corresponding author: Jae Hyuk Lim, jaehyuklim@jbnu.ac.kr

1. Introduction

For several decades, composite materials have been widely used in many industry applications due to their many advantages, such as specific modulus, specific strength, low thermal expansion coefficient, and so forth. To use composite materials in aircraft and spacecraft structures, many studies have been carried out [1].

However, there are noticeable variations in the material properties of the composite material because of voids, resin-rich zones, micro-cracks, and fiber arrangements and various shapes of fibers. Such variations in material properties cause uncertainties in the stiffness and strength of the composite material. Numerous studies have predicted the material behavior of composites by using random fiber distribution models [2-5]. However, there is a drawback that it is not possible to create a model having various fiber shapes, kinking of fibers, and fiber distribution generated by actual manufacturing processes.

In this study, we investigate the variability of material behavior through composite modeling that reflects real microstructures fabricated according to actual manufacturing processes.

2. Preparation of the cross-section images of composites through CT scanning

Using the computed tomography (CT) technique, 507 images are generated from sliced layers of composite specimen as shown in Fig. 1. For the generation of the finite element (FE) model, binary images are generated by a black/white filter after proper segmentation algorithm is applied.

Typically, the fiber waviness of unidirectional (UD) composite materials is low, six representative images are taken along the fiber direction as shown in Fig. 1.

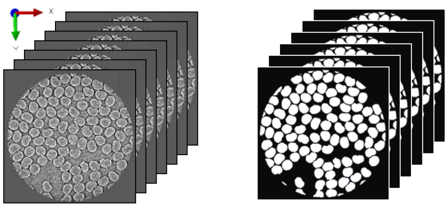
(a) (b)
Fig. 1 Preparation of CT images and binary images: (a) CT images (b) binary images

3. Generation of 3D FE model

A 3D FE model is created from binary images by using the signed distance-based trimmed FE model [6]. First, 2D surfaces containing actual shape are generated by using mesh trimming method as shown Fig. 2. After that, 2D surfaces are connected using CATIA software to generate a 3D solid model. Based on the 3D solid model, a FE model consisting of 270,000 nodes and 2,000,000 tetrahedron elements is generated. Since this FE model is difficult to employ the periodic displacement boundary conditions due to cylindrical outer surface, a modification of FE model is made by cutting out four outer regions as shown Fig. 3.

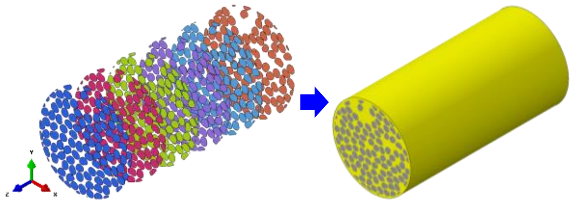
Fig. 2 Generation of 3D CAD in CATIA

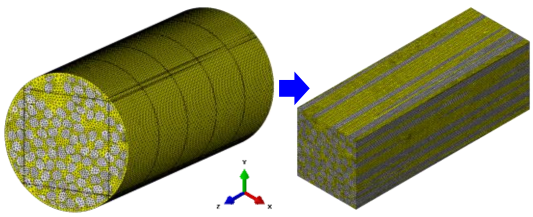
Fig. 3 Generation of a parallelepiped FE model by cutting-out of 3D FE model

4. Results

With the proposed FE model, the equivalent stiffness is predicted using the computational homogenization technique. A set of periodic displacement conditions and material properties in Table 1 are applied and structural analysis is performed. From results, the stiffness matrix and corresponding equivalent properties are obtained.

It is confirmed that a deviation of about 4.6% occurs in the longitudinal elastic modulus from 100 UD random FE models having the same fiber volume ratio (Vf = 0.64) compared to actual microstructure FE model. This is because the microstructural FE model reflects the shape of various fibers and kinked fibers.

5. Conclusion

In this work, we developed a precise FE model generation technique based on CT images of composite specimens. It was confirmed that the actual micro-structure model is kinked at different angles unlike conventional UD composite material with zero kink angles.

From the actual microstructure model and UD random model, a deviation occurs in longitudinal elastic modulus. This is attributed that various fiber shapes and fiber distribution considering kinked fiber are implemented in the FE model.

In the future, we will analyze the fracture behavior difference through various fracture analysis and statistical analysis based on many actual micro-structure models.

Table 1 Material properties of M55J/M18 [6]

Property	M55J(Fiber)	M18(Matrix)
$E33$ [GPa]	496.52	4.2
$E11 = E22$ [GPa]	6.38	4.2
$G12$ [GPa]	2.78	1.5
$G13 = G23$ [GPa]	17.92	1.5
$\upsilon12$	0.25	0.4

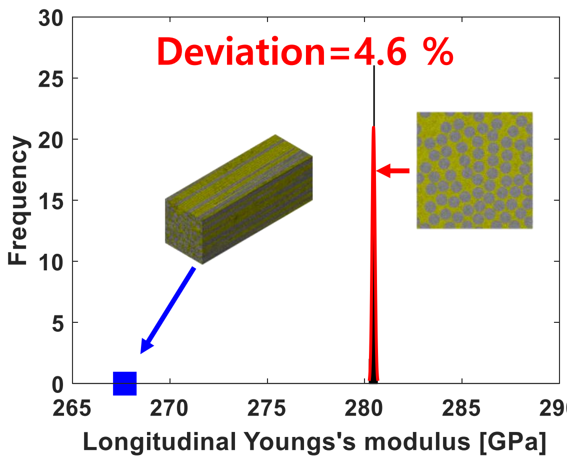

Fig. 4 Comparison of the longitudinal Young's modulus between random and micro-structure FE model

Acknowledgment

This research was supported by the Space Core Technology Development Program through the National Research Foundation of Korea (NRF) funded by the Ministry of Science and ICT (No. 2018M1A3A4A04047087).

References

[1] D. G. Lee, *Composite Materials*, First Ed. Honrung Publishing Company, Seoul, Korea, (2007).

[2] J. H. Lim, Numerical prediction of fiber mechanics properties considering random microstructure using inverse analysis with quasi-analytical gradients, *Applied mathematics and computation*, 273 (2016) 201-206.

[3] G. Li, A new approach to rapidly generate random periodic representative volume elements for microstructural assessment of high volume fraction composites, *Materials & Design*, 150 (2018) 124-138.

[4] S. M. Park, J. H. Lim, Efficient generator of random fiber distribution with diverse volume fractions by random fiber removal, *Composites Part B: Engineering*, 167 (2019) 302-316.

[5] D. W. Kim, J. H. Lim, Efficient prediction of the electrical conductivity and percolation threshold of nanocomposite containing spherical particles with three-dimensional random representative volume elements by random filler removal, Composites Part B: Engineering, 168 (2019) 387-397.

[6] J. H. Lim, A microstructure modeling scheme of unidirectional composites using signed distance function based on boundary smoothing and element trimming, Advances in Engineering Software, 109 (2017) 1-14.